旋網漁具の沈降特性への目合変化の効果

誌名	水産工学
ISSN	09167617
著者	高木, 力 宮田, 俊輔 伏島, 一平 大島, 達樹 上原, 崇敬 鈴木, 勝也 野村, 芳徳 金築, 正道 鳥澤, 眞介
巻/号	51巻1号
掲載ページ	p. 11-19
発行年月	2014年7月

水産工学 Fisheries Engineering
Vol. 51 No. 1, pp. 11～19, 2014

【Research Article】

Effect of Mesh Size on Sinking Characteristics of Purse Seine Net : a Parametric Study by Numerical Simulation

Tsutomu TAKAGI[1]*, Syunsuke MIYATA[1], Ippei FUSEJIMA[2], Tatsuki OSHIMA[2], Takayoshi UEHARA[2], Katsuya SUZUKI[3], Yoshinori NOMURA[3], Masamichi KANECHIKU[1] and Shinsuke TORISAWA[1]

Abstract

We numerically modeled the geometry of a purse seine net and evaluated the model's dynamic behavior during operation. The vessel position, wire payout and roll-up lengths, and current flow speed and direction *in situ* were collected as the dataset for computation. The mesh sizes of the upper, middle, and lower sections of the main net were changed to double and half their respective sizes, and the sinking speed and depth were compared among nets of different mesh sizes. The net with doubled mesh size in the lower section and constant mesh bar diameter strongly affected the sinking speed and depth. This implies that a large mesh size in the lower part of the main net, which eliminates the need for providing a thicker mesh bar, should be used for enhancing the efficiency of fishing operations.

1. Introduction

Large and medium-sized purse seine fishing operations are among the most important fishing operations in Japan because such operations, which mainly target horse mackerel, sardine, skipjack, and yellow fin tuna, account for 27% of Japan's total marine fishing production (900,000 tons)[1)]. For fishing skipjack, big eye, and yellowfin tuna, generally, single, large purse seine fishing vessels operate in exclusive economic zones around island countries in southwest Pacific and east Indian ocean. Specifically, over 70% of skipjack tuna caught in those areas is accounted for by large purse seine fishing vessels.

For far-sea large purse seine vessels, the share of fuel cost in total vessel operating cost is greater than 15%. Therefore, the total load on the ship must be reduced. For instance, by reducing the weight of fishing gear, while improving its performance, we can achieve a decrease operation time and an increase in catch per unit effort (CPUE).

Traditionally, Japanese large single purse seine vessels have used a fish aggregation device (FAD) for efficient fishing, but the FAD has some issues such as trapping small-size fishes and by-catch[2)]. Therefore, it has been suggested that using a larger mesh size for the main purse seine net can help smaller fish escape. In addition, the fishing net would be lighter.

A few pragmatic studies on fish mortality during or after pursing have been carried out by performing experiments *in situ*. Misund and Beltestad[3)]examined the effect of using sorting grids on a purse seine net on the escape of small-sized fish and confirmed an improvement in the survival rate of the escaping fish. Mitchell *et al.*[4)] proved that the high density of *Sardinops sagax* significantly affected their survival rate after rolling over the head line of a purse seine fishing net. Because a purse seine fishing vessel can surround a large shoal of fish within a short period, it is necessary that we grasp the geometries of the entire fishing net, while focusing on some portions for evaluating their functionality during fishing. However, observation of fishing nets *in situ* is difficult given their large size. Thus, a few groups of researchers have attempted to carry out model experiments in large basins or flume tanks[5~8)]. However, there are

Received November 28, 2013, Accepted December 24, 2013
Key words : purse seine net, mesh size, sinking speed, sinking depth
[1] Kinki University, Faculty of Agriculture, 3327-204, Naka, Nara, 631-8505, Japan
[2] Marine Fisheries Research and Development Center, 15F Queen's Tower B, Minato-Mirai, Nishi, Yokohama, 220-6115, Japan
[3] Nitto Seimo Co., Ltd., 14 Ichimonji, Fukuyama, 721-0953, Japan
* Tel : +81-742-43-6169, tutakagi@nara.kindai.ac.jp

some limitations, for example, the flexural rigidity of the netting twines cannot be assured for the model net, and it is difficult to recreate actual operational conditions in the model environment. Therefore, as a countermeasure, the authors have developed a NaLA-based numerical simulation system for recreating the underwater dynamic geometry of a purse seine net during operation. NaLA is a basis of the computer simulation program for estimating the geometry and loads of a universal fishing net[9]. In addition to the author's group, several other researchers have worked on the numerical simulation of a purse seine net. Kim *et al.*[10], conducted numerical simulation for a purse seine net using the mass-spring model and compared the simulation results with field data. Riziotis *et al.*[11] simulated a purse seine net by using the finite element method and compared the simulation results with those of a model experiment. Numerical simulation affords users the advantage of generating many types of purse seine net models with varying design parameters under identical real operating conditions such as current flow and vessel path.

In the present study, in order to assess the basis of possible efficient fishing for increasing the energy savings and enhancing the fish selectivity of purse seine netting operations, a purse seine model was developed based on the design specifications used for the numerical simulation, and the behaviors and geometries of a purse seine net were evaluated by varying the mesh size by using real operating data collected *in situ*.

2. Materials and methods

1) Purse seine net

Fig. 1 shows the grand design of the purse seine net used for the numerical simulation in the present study. This net was used in "Nippon Maru," a single purse seine fishing vessel displacing 744 tons and used mainly for tuna fishing in far-sea areas. The large buoy (diameter: 115 cm), shown in Fig. 1, is cast at the start of the operation and then the purse net is cast for enclosing a shoal of fish. The buoy line, which is connected to the buoy, must be rolled up when surrounding a shoal of fish for retrieving the buoy and the tip end of the net with the end of purse wire. Thereafter, both ends of the purse wire are rolled up to haul the purse seine net. The purse wire is put through the purse rings attached to the bottom of the net. Upon rolling up the purse wire, the bottom side of the net is pursed up for hauling. The purse wire, buoy line wire, and towline wire were paid out by 2142 m, 1019 m, and 406 m, respectively, for the operation. The mesh sizes, twine diameters, and other information pertaining to each net section are summarized in Table 1.

The purse seine net has a wing net on both sides of the main net. A 1740-m-long buoy head line was attached to the top side of the purse seine net. A 1640-m-long sinker line was attached to the bottom side for increasing sinking speed. The main net was divided into three sections, as shown in Fig. 1. The mesh sizes in the upper, middle, and lower sections are 105 mm, 270 mm, and 150 mm, respectively, and the average net densities of those sections were about

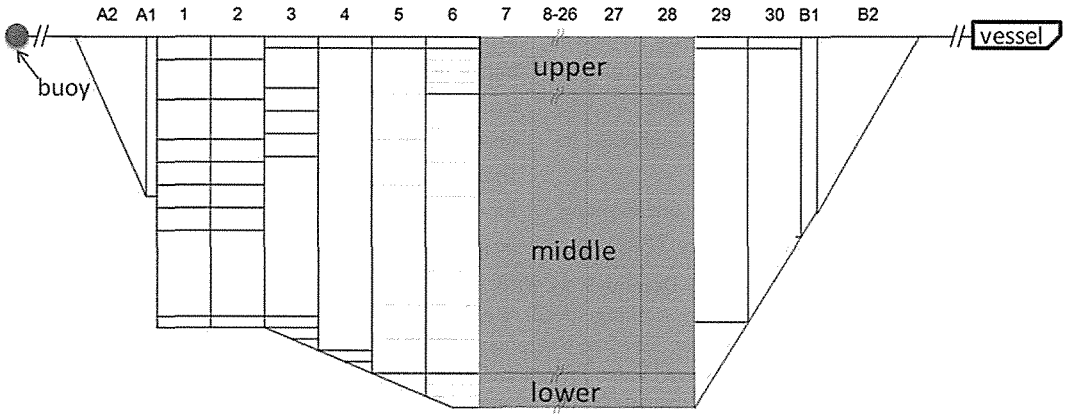

Fig. 1 Design of purse seine net used in actual fishing operations.

Table 1 The mesh sizes, twine diameters, and other information pertaining to each net section.

Region	A2	A1	1	2	3	4	5	6
Number of mesh in depth direction	145	1346	2150	2150	2300	2350	1950	1550
Number of net panel	1	2	22	23	25	25	21	16
Mesh diameter (mm)	7.3	2.4	1.7-3.8	1.4-2.5	1.4-2.8	1.5-2.8	1.5-2.8	1.5-2.8
Mesh size (mm)	360	90	140-320	140-320	120-240	105	105-270	105-270

Region	7	8-26	27	28	29	30	B1	B2
Number of mesh in depth direction	1550	1550	1550	1550	2450	1950	1346	200
Number of net panel	16	16	16	16	25	20	1	1
Mesh diameter (mm)	1.5-2.8	1.5-2.8	1.5-2.8	1.5-2.8	2.6-3.1	2.6-3.1	2.4	7.3
Mesh size (mm)	105-270	105-270	105-270	105-270	105-150	105-150	90	360

$1100kg \times m^{-3}$, $1280kg \times m^{-3}$, and $1190kg \times m^{-3}$ according to the specification sheet. These values were used for our calculations.

2) Operation data

A fishing operation was carried out in the area (1°6' – 6°1' S, 84°50' – 91°28' E) in the east Indian Ocean. The main target species were Skipjack, Bigeye, and Yellowfin tuna. The fishing was conducted from Oct 29, 2012, to Dec 8, 2012. The trajectory of the vessel during fishing was recorded by a GPS sensor at 1-s intervals, as well as the instants of the start and end of paying out and rolling up of the purse wire, towing wire, and buoy line wire, The speed and direction of current flow were recorded. There is no device for measuring the payout and roll-up length of the wires at the winches, so video cameras were installed near the winch for observing its rotation. For estimating the average payout or roll-up speed, the total wire length was divided by the time the winch was in rotation from the video images. Variations in the winch speed could not be observed owing to the lack of adequate resolution and the large camera-winch distance. For the validating the simulation results, the depth sensor (model) was set below the center of the main net for obtaining the time series data of depth. The dataset of an operation that was implemented perfectly and yielded an adequate catch was used for the numerical simulation.

The operation dataset used for the numerical simulation is summarized in Table 2. This dataset

Table 2 Dataset of purse seine fishing operation used for numerical simulation.

Elapsed time	Position X	Position Y	Speed of vessel	Heading angle	Pay out length of purse wire winch A	Pay out length of purse wire winch B	Pay out length of towing wire	Pay out length of buoy line	Depth of the sea bottom	Current flow speed (<50m)	Current flow direction (<50m)	Current flow speed (50-100m)	Current flow direction (50-100m)	Current flow speed (50-100m)	Current flow direction (50-100m)
(s)	(m)	(m)	(ms^{-1})	(°)	(m)	(m)	(m)	(m)	(m)	(ms^{-1})	(°)	(ms^{-1})	(°)	(ms^{-1})	(°)
0	0	0	0	22	5	0	0	5	1000	0.1	221	0.3	154	0.2	210
1	1.45	5.25	5.4	21	10.4	0	0	8.6	1000	0.1	221	0.3	154	0.2	210
2	3.01	11.16	6.1	21	16.6	0	0	12.1	1000	0.1	221	0.3	154	0.2	210
3	4.80	16.85	6.0	20	22.5	0	0	15.7	1000	0.1	221	0.3	154	0.2	210
4	6.25	22.43	5.8	20	28.3	0	0	19.2	1000	0.1	221	0.3	154	0.2	210
5	7.37	27.68	5.4	19	33.7	0	0	22.7	1000	0.1	221	0.3	154	0.2	210
6	8.93	32.92	5.5	19	39.1	0	0	26.3	1000	0.1	221	0.3	154	0.2	210
7	10.83	37.83	5.3	18	44.4	0	0	29.8	1000	0.1	221	0.3	154	0.2	210
8	12.83	42.74	5.3	18	49.7	0	0	33.3	1000	0.1	221	0.3	154	0.2	210
9	14.95	47.43	5.1	17	54.8	0	0	36.9	1000	0.1	221	0.3	154	0.2	210
10	16.85	52.34	5.3	17	60.1	0	0	40.4	1000	0.1	221	0.3	154	0.2	210
11	18.41	57.47	5.4	16	65.5	0	0	44.0	1000	0.1	221	0.3	154	0.2	210
12	19.42	62.94	5.6	15	71.0	0	0	47.5	1000	0.1	221	0.3	154	0.2	210
13	19.98	68.63	5.7	15	76.8	0	0	51.0	1000	0.1	221	0.3	154	0.2	210

consists of the vessel location ; vessel speed; vessel course ; payout lengths of the purse wire, tow line wire, buoy-line wire ; sea water depth ; and speed and direction of current flow recorded at 1-s intervals.

3) Numerical simulation

The numerical simulation model used in this study was developed by the authors in previous studies[12)~15)] and applied to a gill net[16), 17)], Danish seine net[18)], and an aquaculture net cage[19)]. The model is a lumped mass model in which the net and the lope were assumed as being composed of masses and springs. Fig. 2 shows a schematic view of the model used for the computation. Generally, the forces acting on the net and other rigs of the fishing gear are gravitational, buoyant, hydrodynamic, and internal tension. These forces balance the inertia forces, and the balance can be expressed as the equation of motion. This equation is written as follows[15)] :

$$\left(\mathbf{M}_i+\sum_{K=1}^{2}\left[\mathbf{C}_{ik}\cdot\Delta\mathbf{M}_{ik}\cdot\mathbf{C}_{ik}^{T}\right]\right)\vec{\alpha}_i = \vec{T}_i+\sum_{k=1}^{2}\left(\mathbf{C}_{ik}\cdot\vec{F}_{ik}\right)+\vec{W}_i+\vec{B}_i \quad \cdots\cdots(1)$$

Here, $\mathbf{M}_i$ denotes the mass, $\Delta\mathbf{M}_{ik}$ is the added mass, F_{ik} is the drag, W_i is the weight, B_i is the buoyancy, and T_i is the tension force.

The body-fixed coordinate system for the net elements allows for the easy estimation of fluid force. This is because if the fluid force acting on a net bar element is divided into the normal and the tangential force, constant fluid dynamic coefficients can be applied without considering the flow direction. The forces acting on the net bar elements can be consolidated into mass points and the moments assumed as not being considered. Similarly, the external force on a net panel element can be consolidated at its vertexes; thus, the uniform approach can be applied, and the same formulation can be used for the computational algorithm.

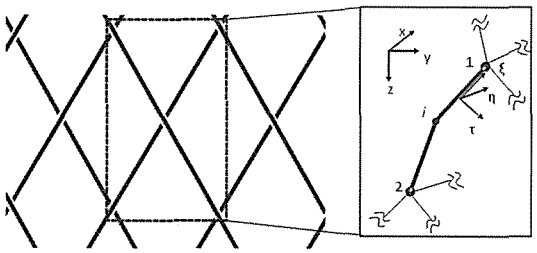

Fig. 2 Numerical model simulating geometry of and loads on fishing gear.

The inertia transformation matrix, $\mathbf{C}_{ik}$, in equation (1) has to be used for transforming the body-fixed coordinate system into the global coordinate system. The velocity and position at every time step can be computed by numerically integrating equation (1) using the sixth-order Runge-Kutta method.

4) Purse seine net design parameters

For evaluating the effects of mesh size on sinking speed and depth, different net types with varying mesh sizes were used. The original mesh sizes of the upper (105mm) , middle (270mm) , and lower (150mm) sections were changed to half (upper, middle, lower = 52.5mm, 135mm, 75mm) and double (210mm, 540mm, 300mm) their original sizes. Thus, 27 different mesh size combinations were available for assessing the sinking characteristics of the net through numerical simulation. Additionally, when the mesh size was changed, we provided both types of nets, i.e., that with constant mesh bar diameter and that with constant projected net area. Therefore, 54 different purse seine main net configurations were available for numerical simulation.

3. Results and discussion

1) Simulation results of original purse seine net using actual operation data

The trajectory and events during the operation are shown in Fig. 3. The time elapsed between casting of the net and pursing was 2080 s and that between casting and finishing the net was 319 s. Thereafter, 1400 s was required for pursing the net. The computation was performed under the conditions of the operation dataset summarized in Table 2. The

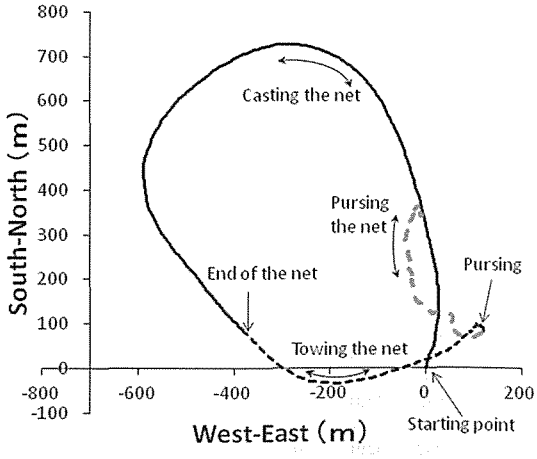

Fig. 3 Track of purse seine boat.

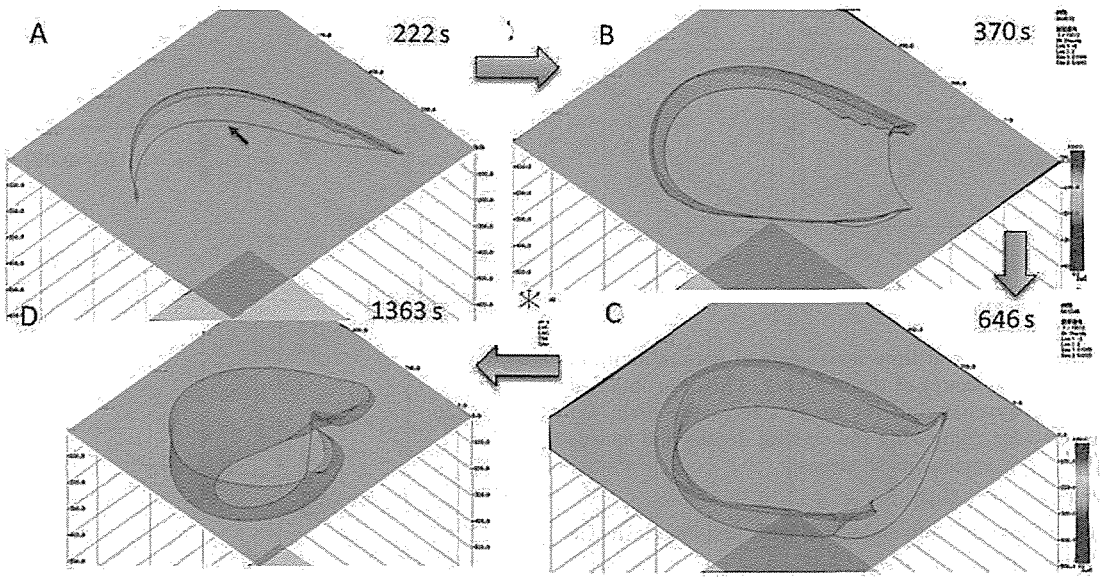

Fig. 4 Geometry of purse seine net during fishing operation with numerical simulation. The track and current profile datasets were used for facilitating computations.
A, during operation ; B, end of casting; C, start of pursing ; D, during pursing. The arrow indicates the buoy line wire.

numerical simulation result is shown in Fig. 4.

In the simulation result, the loads acting on and the geometry of the net were obtained as the numerical dataset, and these data are visualized using a viewer. The viewer can grasp not only the entire net but also its dynamic behavior and a close-up of its mesh geometry.

2) Validity of simulation result

This simulation system has already been applied to many fishing gears, and we validated the simulation system in almost all of our previous works. However, here, we have compared the simulation results with data from an actual operation. The time series data of the depth sensor set below the center of the main net and the simulation data of the same point at the net are shown in Fig. 5.

The maximum sinking depth of the actual net was 152 m at 1110 s after casting. The simulation result provided good agreement with the actual data, particularly more so until 1000 s from the point of casting the net. In purse seine fishing, fishermen have a strong notion of how quickly a shoal of fish can be surrounded. Therefore, the agreement between the simulated and actual net sinking profiles is very important for evaluating purse seine net behavior. In contrast, after reaching the maximum depth, some fluctuations can be seen in the simulation results. These fluctuations could possibly be ascribed to the characteristics of the lumped mass model. For solving this problem, strong dampers should be provided to compensate for the cases of expansion and contraction of the bar elements. However, the additional stiffness may prolong the computation time. Thus, this option cannot be considered for practical use. The difference between the simulated and actual profiles during rolling up the purse wire can be seen. It may be caused by the inaccurate winch speed for the computation because changes in the winch speed could not be observed due to the lack of adequate resolution of the video camera. The accurate data can therefore reduce the difference between the profiles.

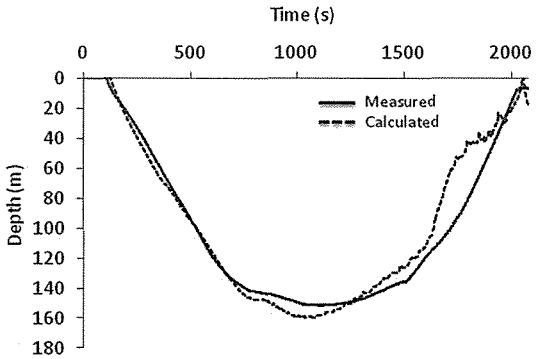

Fig. 5 Comparison of measured and computed depths of purse seine net center.

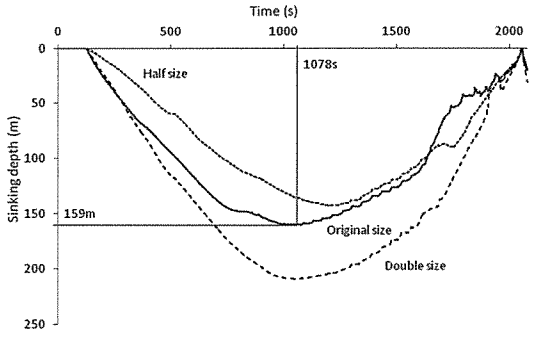

Fig. 6 Profile of time series data of bottom depth of the center of the main net. This was obtained by changing the mesh size of the main net for comparing the sinking depths and speeds of various mesh sizes.

3) Sinking depth and speed with varying mesh size

(1) Constant mesh bar diameter

Fig. 6 shows the time series data of the depth profile sensor below the center of the main net for the deepest-sinking, shallowest-sinking, and original nets. The mesh of the deepest-sinking net was double in size compared with the original mesh in all sections (upper, middle, and lower) with a constant mesh bar diameter. The maximum sinking depth was 209 m at 1053 s after casting. In contrast, the meshes of the middle and lower sections of the shallowest-sinking net were half the size of the original mesh; the upper section retained the original mesh size. The maximum sinking depth was 134 m at 1204 s after casting. The average sinking speeds of the original, deepest-sinking, and shallowest-sinking nets were 0.15m·s^{-1}, 0.20m·s^{-1}, and 0.11m·s^{-1}, respectively. In case of the deepest-sinking net, the time required for reaching the maximum depth of the original net (159m) was 694 s, which is 30% faster than the original net. This means that a large mesh size allows for faster sinking to the desired depth, thus reducing the operation time.

The mesh sizes of each section (upper, middle, and lower sections) were changed to half and double the original size; therefore, 27 mesh size combinations, including original mesh size, were available for comparing the simulation results. The sinking speeds in those cases are plotted for each mesh size combination in Fig. 7. For instance, if we consider one mesh size of the upper section, because the mesh size was the half, double and original size in each section, eventually 3′3 points were marked on the same mesh size.

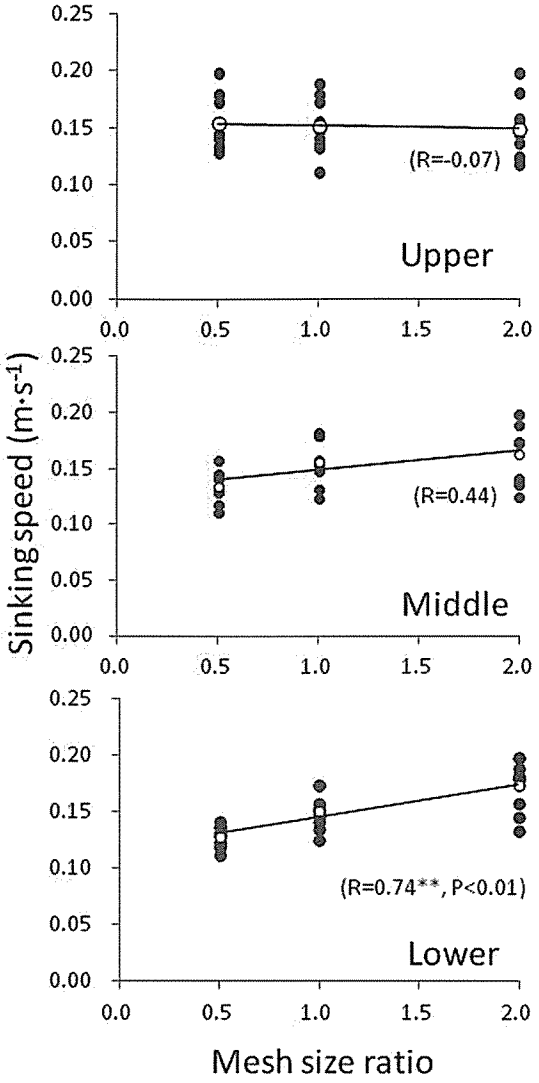

Fig. 7 Sinking speed vs. mesh size for main net of purse seine with constant mesh bar diameter. Mesh size ratio was obtained by dividing the mesh size by the original size. The mesh size of the net' s lower section significantly affected its sinking speed (R=0.74 ; p<0.01).

The averaged values of the sinking speeds for the same mesh size were estimated, and regression lines were drawn for each net section, as shown in Fig. 7. The gradients of these regression lines indicate the sensitivity of sinking speed to mesh size. From the results, the mesh size of the upper section did not affect the sinking speed of the main net. In contrast, the mesh size of the lower section did strongly affect the speed, as indicated by the large gradient of the corresponding regression line (R=0.70 ; p<0.01). This implies that a large mesh size leads to quick sinking of

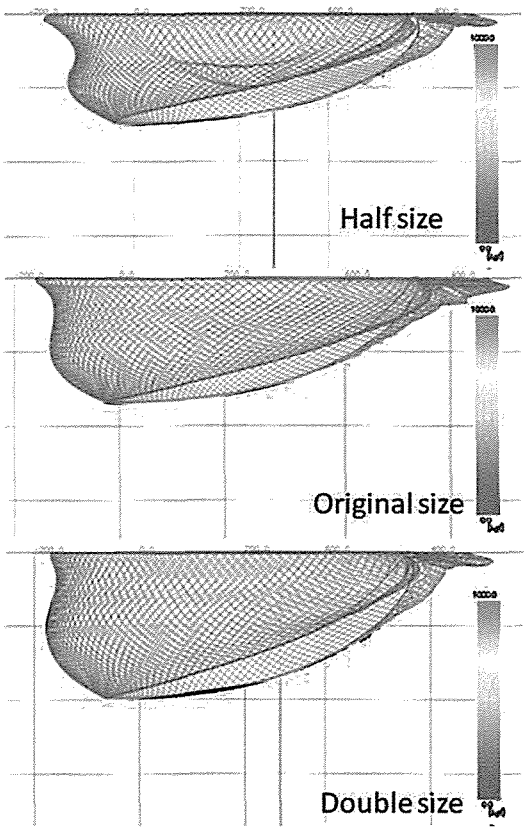

Fig. 8 Side view of purse seine net for various mesh sizes of lower section with constant mesh bar diameter, after 1100 s of casting.

the main net. Additionally, in terms of sinking speed, the vertical region of a large-sized mesh is the key factor rather than the area of the net large-sized mesh.

Fig. 8 shows the side view of the purse seine net as the mesh size of the lower section is varied. The mesh size of the lower section remarkably affected the net' s vertical deployment. The inner volume surrounded by the net with the largest mesh size was the largest among all cases. This substantiated that the large mesh size in the lower section was effective for faster sinking of the net and surrounding of target.

(2) Constant projection area of main net

Sinking speeds were compared by changing the mesh size while maintaining a constant projection area equal to that of the original main net, as shown in Fig. 9. While the mesh size of the upper section did not affect the sinking speed, those of the middle and lower sections influenced the net' s sinking speed. The regression lines were drawn in the same manner as those of Fig. 7, and the sinking speed showed the most

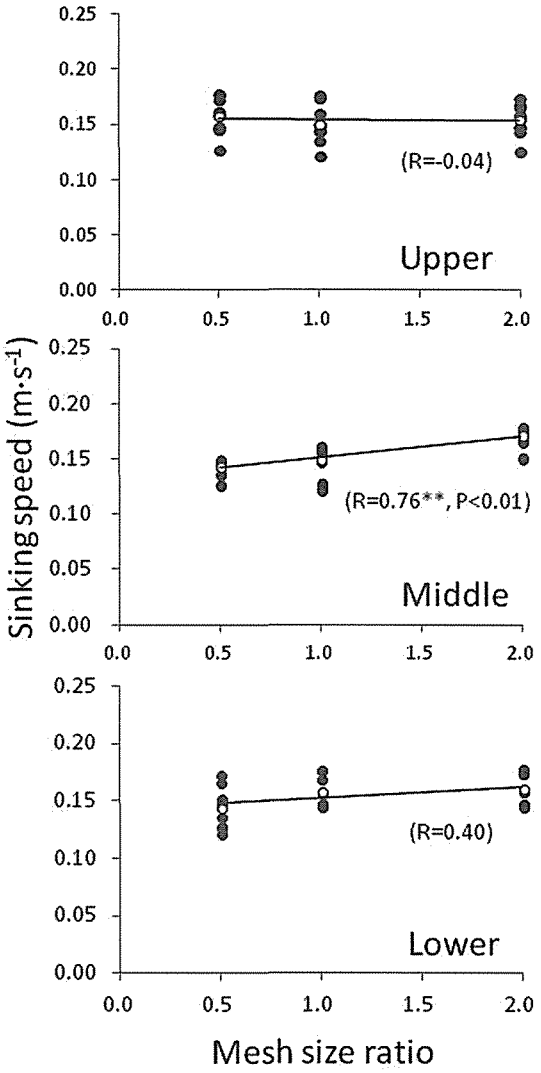

Fig. 9 Sinking speed vs. mesh size of main net of purse seine with constant projected area of main net. The mesh size of the net's middle section significantly affected the sinking speed (R=0.76 ; p<0.01).

sensitivity toward the mesh size of the middle section (R=0.76 ; p<0.01). Variations in the data plots of the upper section were greater than variations in the plots of other sections, whereas variations in the data plots of the middle section were smaller than those in the plots of other sections. This implies that under a constant projection area, the effect of mesh size on sinking speed is the greatest in the middle section.

In the case of double mesh size in the middle section with original size in the other sections, the maximum sinking depth was 186 m at 1052 s, and the averaged sinking speed was 0.177m·s^{-1}. The corresponding

values for the original net were 159 m, 1078 s, and 0.145m·s^{-1}. The sinking speed and the maximum sinking depth were 20% and 17% greater than the respective values of the original net. In contrast, previously, with double mesh size in the lower section and constant mesh bar diameter, the maximum depth and the averaged speed were 189m and 0.180m·s^{-1}, respectively. The net area of the lower section was smaller than that of the middle section; thus, this means that if the mesh size of the net' s lower section can be increased while not changing the mesh bar diameter, faster sinking speeds can be achieved in an effective manner. However, because the load of the purse seine wire during pursing acts directly on the lower section of the main net, the mesh size of the lower section should not be enlarged excursively. Therefore, assuming adequate strength against acting loads, the use of a large-sized mesh size in the lower section of the main net is effective for fast encircling and efficient operation. In addition, the weight of the fishing gear is reduced, and small fish can easily escape through the net. A simulation study such as this one helps create and implement new design and operation schemes for mitigating the impact of fishing.

References

1) Ministry of Agriculture, Forestry and Fisheries of Japan: Statistics of Agriculture, Forestry and Fisheries in 2012. pp. 1-31, 2013.
2) J. W. Valdemarsen: Technological trends in capture fisheries. *Ocean & Coastal Management*, 44 : 635-651, 2001.
3) O. A. Misund and A. K. Beltestad: Survival of mackerel and saithe that escape through sorting grids in purse seines. *Fisheries Research*, 48 : 31-41, 2000.
4) R. W. Mitchell, S. J. Blight, D. J. Gaughan and I. W. Wright: Does the mortality of released Sardinops sagax increase if rolled over the headline of a purse seine net? *Fisheries Research*, 57 : 279-285, 2002.
5) Y. Iitaka: Model Experiments on the Sardine Purse Seine Operating in Hiuganada.-I. *NIPPON SUISAN GAKKAISHI*, 20 : 571-575, 1954.
6) T. Konagaya : Studies on the purse seine-I effect of the pursing velocity. *NIPPON SUISAN GAKKAISHI*, 32 : 507-510, 1966.
7) D. Liu, O. Sato, K. Nashimoto and K. Yamatomo: Configuration of Leadline of Purse Seine. *BULLETIN OF THE FACULTY OF FISHERIES HOKKAIDO UNIVERSITY*, 35 : 234-242, 1984.
8) J. Shin, T. Imai, S. Fuwa and M. Ishizaki : A Model Experiment on the Characteristic of Fishing Gear of Lampara Net with Various Hanging Ratios. *NIPPON SUISAN GAKKAISHI*, 65 : 33-41, 1999.
9) T. Takagi, K. Suzuki, S. Torisawa, K. Komeyama, M. Kadota and S. Asaumi: Application of NaLA: From Study to Practical Use. *Contributions on the Theory of Fishing Gears and Related Marine Systems*, 7 : 261-271, 2011.
10) H.-Y. Kim, C.-W. Lee, J.-K. Shin, H.-S. Kim, B.-J. Cha and G.-H. Lee: Dynamic simulation of the behavior of purse seine gear and sea-trial verification. *Fisheries Research*, 88 : 109-119, 2007.
11) V. A. Riziotis, G. M. Katsaounis, G. Papadakis, S. G. Voutsinas, G. Bergeles and G. D. Tzabiras: Numerical and experimental analysis of the hydroelastic behavior of purse seine nets. *Ocean Engineering*, 58 : 88-105, 2013.
12) T. Takagi, T. Shimizu, K. Suzuki, T. Hiraishi, Y. Matsushita and T. Watanabe: Performance of "NaLA" : a fishing net shape simulator. *Fisheries Engineering*, 40 : 125-134, 2003.
13) T. Takagi, T. Shimizu, K. Suzuki, T. Hiraishi and K. Yamamoto: Validity and Layout of "NaLA" : a Net Configuration and Loading Analysis System. *Fisheries Research*, 66 : 235-243 2004.
14) T. Takagi, K. Suzuki and T. Hiraishi: Modeling of net for calculation method of dynamic fishing net shape *Fisheries Science* 68 : 1857-1860, 2002.
15) T. Takagi, T. Shimizu and H. Korte: Evaluating the impact of gillnet ghost fishing using a computational analysis of the geometry of fishing gear. *ICES Journal of Marine Science* 64 : 1517-1524, 2007.
16) T. Shimizu, T. Takagi, H. Korte, T. Hiraishi and K. Yamamoto: Application of NaLA, a fishing net configuration and loading analysis system, to drift gill nets. *Fisheries Research*, 76 : 67-80, 2005.
17) T. Shimizu, T. Takagi, H. Korte, T. Hiraishi and K. Yamamoto: Application of NaLA, a fishing net configuration and loading analysis system, to bottom gill nets. *Fisheries Science*, 73 : 489-499, 2007.
18) K. Suzuki and T. Takagi: Numerical analysis of dynamic behavior of Danish seining and sea trial verification. *Mathematical and Physical Fisheries Science*, 6 : 11-22, 2008.
19) K. Suzuki, S. Torisawa and T. Takagi: Numerical Analysis of Net Cage Dynamic Behavior Due to Concurrent Waves and Current. *Proceedings of the ASME 28th International Conference on Offshore Mechanics and Arctic Engineering OMAE2009*, OMAE2009-80078, 2009.

【研究論文】

旋網漁具の沈降特性への目合変化の効果:
数値シミュレーションによるパラメトリックスタディー

高木　力[1]*・宮田俊輔[1]・伏島一平[2]
大島達樹[2]・上原崇敬[2]・鈴木勝也[3]
野村芳徳[3]・金築正道[1]・鳥澤眞介[1]

和文要旨

大型まき網の操業時の水中形状を数値計算によってシミュレーションし,漁具形状の動的特性を評価した。身網の区画を上層，中層，下層の三区画に分割し，各区画の目合をオリジナルとその2倍および半分に変化させ，網地の沈下特性を比較した。網糸直径を一定にして目合を変化させた場合は，下層の網地の目合の違いが最も沈降速度と深度に影響を与えた。網糸の太さを変えずに,下層の網地の目合を大きくすることによって沈降速度が増加することになり，操業の効率化が期待できる。

2013年11月28日受付，2013年12月24日受理
キーワード：旋網，目合，沈降速度，沈降深度
[1] 近畿大学農学部，〒631-8505奈良県奈良市中町3327-204
[2] (独) 水産総合研究センター開発調査センター，〒220-6115, 神奈川県横浜市西区みなとみらい2-3-3クイーンズタワーB15F
[3] 日東製網株式会社，〒721-0953, 広島県福山市1一文字町14
*Tel：+81-742-43-6169, tutakagi@nara.kindai.ac.jp